Appl. Phys. A 63, 257–265 (1996)

Applied Physics A Materials Science & Processing

© Springer-Verlag 1996

Comparison of the transmission behavior of a triazeno-polymer with a theoretical model

T. Lippert[1,*,], L.S. Bennett[2], T. Nakamura[1], H. Niino[1], A. Ouchi[1], A. Yabe[1]**

[1]National Institute of Materials and Chemical Research, Laser Induced Reaction Lab, Higashi 1-1, Tsukuba, Ibaraki 305, Japan
[2]National Institute of Materials and Chemical Research, Energetic Materials Lab, Higashi 1-1, Tsukuba, Ibaraki 305, Japan

Received: 5 December 1995/Accepted: 30 May 1996

Abstract. The threshold fluence, F_{Th}, of ablation of a triazeno-polymer was measured in the low fluence range for thin films using conventional UV-spectroscopy. It was found that there is a clearly defined F_{Th} for 308 nm irradiation between 20 and 25 mJ cm^{-2}. In the case of 248 nm irradiation, a "threshold fluence range" between 16 and 32 mJ cm^{-2} was found. The ablation rate for both irradiation wavelengths depends on film-thickness. For the XeCl excimer-laser, the point at which the rate becomes independent of thickness was observed to lie at a value which did not correspond to the calculated laser penetration depth, whereas for the KrF laser the independence was not reached within the applied thickness range (up to 0.35 μm). Additional transmission measurements have been performed showing that the target transmission at 248 nm increases only slightly, whereas for 308 nm the transmission increases by a factor of approximately 4. This result shows that dynamic target absorption properties are very important for describing the ablation process. The results derived from the transmission studies and etch rates were analyzed theoretically with a two-level model of chromophore absorption. For 248 nm irradiation this model can describe the transmission behavior and the ablation rate. In the case of 308 nm irradiation, it was only possible to match one data set. A good agreement with the experimental transmission ratio does not match the ablation rate and vice versa.

PACS: 81.60; 42.10; 82.50

Since the first reports about etching of organic polymers [1,2] using pulsed UV lasers, numerous studies [3,4] have been published. Applications include surgery [5–8] and image transfer [9,10]. To optimize pulsed UV laser ablation of polymers one must understand the mechanism of ablation. This would allow determination of optimum processing parameters and material properties for the desired application. Development of a model could eliminate the need for time consuming studies of each polymer at every wavelength for all times scales. Currently this goal has not been achieved. The mechanism of ablation still remains partly unclear. There are mainly two mechanisms for the first step of ablation: *photochemical* and *photothermal*. Which of the two pathways is acting or whether a mixture of both is the real driving force of ablation in polymers remains a point of controversy.

One approach to distinguish between the two pathways was the development of a novel class of photopolymers designed for ablation at 308 nm [11,12]. The investigations showed that the concept of designing polymers for laser ablation at specific wavelengths is feasible. These polymers are photolabile. Photolysis leads to the production of small molecules, like N_2, which can act as the driving force for material removal and provide the gas to transport material away from the ablation region. These properties of the polymer resulted in high resolution etching of one chosen polymer at 308 nm [12].

Various models have been developed to describe the influence of thermal aspects on the ablation characteristics. Arrhenius-type rate expression [13], thermal diffusion [14] and a model assuming one dimensional heat transfer after the two-level chromophore absorption show good agreement with experimental data [15].

In recent studies of a photochemical model, attention was drawn to the absorption properties of the polymer during the laser pulse [16,17]. These results were analyzed theoretically using a "two-level" model of chromophore absorption [18]. In this model, excited states of the chromophore are capable of photon absorption. The model is shown in scheme 1. In Equations 1 and 2 the single photon absorption for ablation depth and

*Author to whom correspondence should be addressed

**Present address*: Los Alamos National Laboratory, Division of Chemical Science and Technology, CST 6, MS-J 585, Los Alamos, New Mexico 87545, USA
Fax: 505-665-4817, E-mail: lippert@lanl.gov

transmission ratio is described,

$$d = \frac{1}{\rho}(S_0 - S_{th}) + \frac{1}{\rho\sigma_1}\ln\left(\frac{1 - e^{-\sigma_1 S_0}}{1 - e^{-\sigma_1 S_{th}}}\right) \quad (1)$$

where d = the etch rate, S_0 = photon density striking the surface target, S_{th} = photon density at the threshold fluence, ρ = chromophore density and σ = absorption cross-section.

$$\frac{T_H}{T_L} = \frac{e^{(\rho\sigma_1 d)}}{\sigma_1 S_0}\ln\left(1 + \frac{e^{(\sigma_1 S_0)} - 1}{e^{(\rho,\sigma_1 d)}}\right) \quad (2)$$

In Eq. 2 T_H is the transmission of the laser pulse at various fluences, T_L = transmission of the sample measured with low energy, e.g. a UV-Vis spectrometer.
The model can be extended to two-levels of excited states (Scheme 1), as described in Eq. 3

$$\frac{dS}{dx} = -\rho\sigma_1 S - \rho\frac{\sigma_1 - \sigma_2}{\sigma_1}[1 - e^{(-\sigma_1 S)}] \quad (3)$$

where S = photon density in the laser pulse (F/h), x = depth in the target, σ_1 = absorption cross-section of the first excited state, σ_2 = absorption cross-section of the second excited state.
The absorption cross-sections can be calculated according to (4),

$$\alpha_{lin} = \rho * \sigma \quad (4)$$

where ρ = chromophore density and σ = absorption cross-section.

The chromophore density can be calculated according to (5)

$$\rho = n * \rho. \quad (5)$$

where ρ = chromophore density, n = number of chromophores and ρ_m = the monomer density.

In this paper we describe our experiments to probe this photochemical model with the same photolabile triazeno-polymer (structure shown in scheme 2) as in Ref. [12]. In addition we applied semiempirical calculations to determine a realistic number of chromophores, which results in decreasing number of "free" fitting parameters.

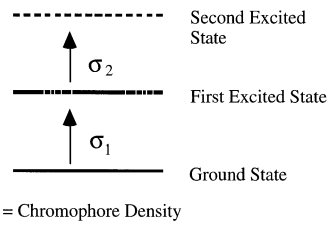

Scheme 1. Theoretical chromophore absorption model to analyze the dynamic absorption of the triazenopolymer. Initially the polymer chromophores are in the ground state with the chromophore density ρ. Absorption of photons from the laser pulse promotes some chromophores to the first and second excited state. The absorption cross-section of both are indicated with σ_1 and σ_2

1 Experimental Methods

Material. The polymer was synthesized according to a procedure described elsewhere [19]. The Bis-triazeno model compound, used for the semiempirical calculations (shown in scheme 3), was synthesized and characterized according to Ref. [20].

Thin films of variable thickness were prepared using the solvent cast technique with spectroscopic grade solvent (chloroform, Aldrich). The films were cast on quartz wafers of 5 cm diameter and 2.2 mm thickness. The homogeneity of the films was tested by recording the UV spectra at different positions of the wafer with a spatial resolution of 5 mm.

Instruments. Irradiation of the polymer films was carried out using a Lambda Physik EMG 102 MSC excimer laser at 308 nm and a Lambda Physik EMG 201 MSC excimer laser at 248 nm. The energy was measured with a Gen-Tec joule meter, model ED 500. The UV spectra were recorded on a Shimadzu UV 2100 spectrometer.

The sample transmission was measured using a Hamamatsu photo tube, type R 1193 U-95, which was equipped for the irradiation at 248 nm with an additional filter, Hamamatsu E 3331. A Stanford Research System Instrument, model DG 535, four channel digital delay/pulse generator was used as trigger source. The pulse was recorded with an Iwatsu TS 8123 storage scope which was connected to a RIKEN Denshi Co. recorder.

The film thickness was determined with a Sloan Dektak 3 profilometer.

Data collection procedure

1. Threshold fluence determination and film thickness dependence.
The change in absorbance ΔA after irradiation was obtained from the spectra recorded by the UV-spectrometer. The ΔA value was measured at the absorption maximum (330 nm) 2-3 times for every film. The reason for using the absorption maximum is that this absorption is due to the triazeno chromophore which is thought to decompose first during the irradiation [12]. The values of ΔA were normalized with the fluence to show more clearly the fluence

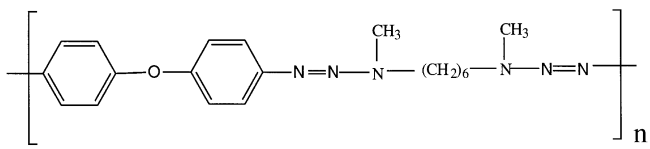

Scheme 2. Chemical structure of the triazenopolymer

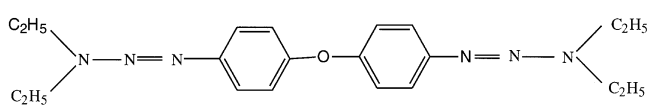

Scheme 3. Structural unit of the Bis-triazeno model compound

at which the absorption changes. A constant film thickness of 0.21 μm was used for the calculation of $\Delta A/F$ for 308 nm and 248 nm to compare both plots directly.

2. Transmission studies.
The single shot transmission of the laser pulse (T_H) was measured at various fluences. At each fluence, the pulse shape and height was averaged over ten to twenty pulse with a quartz wafer at the sample position as illustrated in the experimental set up shown in scheme 4. The fluence was adjusted by varying the sample position relative to the fixed positions of the lens and photo tube. Five to 10 films with various thicknesses were prepared, and the transmittance for a film of given thickness was measured 2–4 times. The sample transmission was analyzed using the simple peak amplitude because no large pulse distortions were detected and the use of the integral of the pulse did not alter the results. The low intensity value of transmission was measured for all films with a conventional UV spectrometer. This value is called T_L in agreement with Ref. [18]. Plots of T_H vs. T_L are linear as shown in Fig. 1. For each fluence the value T_H for a fixed film thickness of 0.1 μm was calculated and used for the plots of the ratio T_H/T_L vs. the applied fluence F. For 248 nm irradiation, linear plots of $T_H$vs. T_L are obtained also.

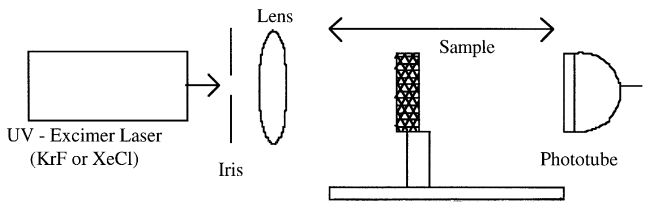

Scheme 4. Experimental set-up for the transmission studies

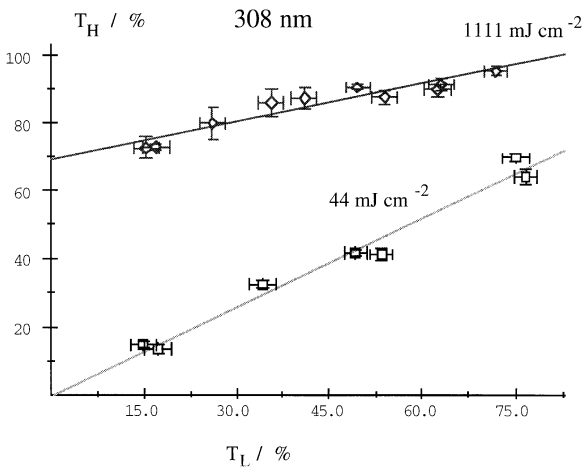

Fig. 1. Linear plot of the transmission value at low energy T_L, derived from a UV spectrometer, vs. the values measured with the laser experiment (T_H). Two different fluences (1.11 J cm^{-2} and 44 mJ cm^{-2}) are shown. The higher fluence represents the case of chromophore saturation, whereas the lower fluence shows the linear transmission behavior (see Fig. 6)

2 Results and Discussion

To be able to apply the photochemical model for the triazenopolymer it was necessary to determine various parameters, such as the monomer density, the linear absorption coefficient and threshold fluence.

2.1 Measurement and Calculation of the Model Parameters

Material constants. To analyze the ablation characteristics in more detail, some material constants were determined. The absorption coefficient of the films was obtained using films of varying thickness measured with a profilometer. Linear regression analysis of the calculated values from the various thick films yielded an absorption coefficient, α_{lin} of 166 000 cm^{-1} at 308 nm and 66 000 cm^{-1} at 248 nm. The density of the polymer was measured by floating the polymer in solutions with various wt% of NaI in water from which a value of about 1.16 g cm^{-3} was determined. Using these values a monomer density of $1.9 \cdot 10^{21}$ cm^{-3} can be calculated.

Threshold of ablation. We decided to re-characterize the threshold fluence (F_{Th}) for thin films, because for the transmission measurements thin films were used. In addition, the previous value was calculated from a linear plot of the etch depth $d(F)$ vs. In F according to

$$d(F) = \frac{1}{\alpha_{eff}} * \ln\left(\frac{F}{F_{th}}\right) \tag{6}$$

where F = the laser fluence in mJ cm^{-2}. The effective absorption coefficient, α_{eff}, during ablation is calculated from the slope of these plots, whereas F_{Th} is the intercept with the x-axis. With this method, the etch depth and energy are normally averaged over many pulses due to the pulse energy deviation of the laser (up to 20%) and the relative high energies applied. The use of the higher fluences results in ablation depths which can be measured more accurately, but small variations of the slope result in quite large uncertainties in the threshold fluence.

This variation is one of the reasons why other investigations have applied a quartz micro balance (QMB) [21, 22] technique to measure the threshold with a much higher precision. As an alternative technique, conventional UV-spectroscopy is used in this study to determine the ablation threshold with single pulses. The absorbance of thin polymer films cast on quartz wafers were measured before and after irradiation with various fluences, as shown in Fig. 2. For all of the measurements, only single pulses on fresh areas of film were used, in order to exclude the influence of chemical (incubation) or physical (microstructures) changes due to successive pulses. The change of the absorbance, ΔA, after irradiation was normalized for the different fluences, $\Delta A/F$. Figure 3 and Fig. 4 show the change of the absorbance, $\Delta A/F$, as a function of laser fluence for 248 and 308 nm irradiation respectively. The data were acquired for a film thickness of 0.21 μm. Linear rather than logarithmic axes are chosen for a more detailed view of the absorbance changes. The reason for choosing this particular film thickness will be discussed later.

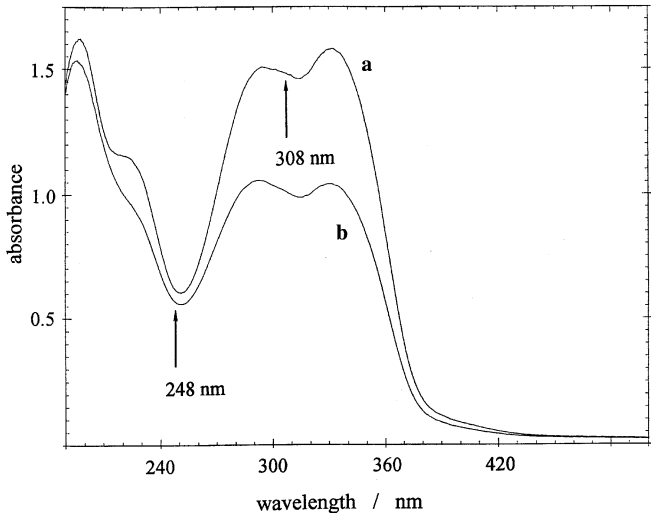

Fig. 2. UV absorption spectra of a thin polymer film (about 0.2 μm) on a quartz wafer before (**a**) and after irradiation (**b**) with a single pulse of 30 mJ cm^{-2} at 308 nm. This value represents a fluence above the threshold of ablation and the change of the absorbance corresponds to ablation. As evident from the figure, 248 nm corresponds to an absorption minimum, whereas 308 nm is close to the absorption maximum

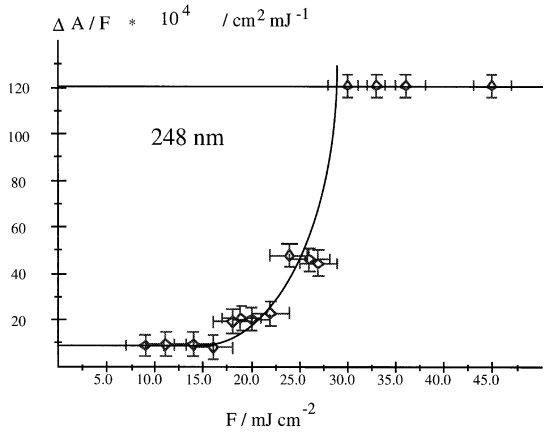

Fig. 3. Plots of the change of absorbance ΔA of thin polymer films (0.21 μm), recorded before and after single pulse irradiation with 248 nm. The values are normalized with the applied fluence and plotted vs. the fluence. A nearly exponential increase is detected between 16 and 28 mJ cm^{-2}

The threshold fluence is defined as the fluence where a sudden increase of $\Delta A/F$ is observed. A comparison of the $\Delta A/F$ values calculated from these experiments using thin films and of those calculated from experiments done in solution reveals different behaviors. In solution the change of the absorbance in the applied fluence range is smaller than those in the films, and no sudden increase was observed. For the solution experiments approximately the same beam size and same absorption was used as for the thin films. The only difference is the pathlength of the beam through the film (100 to 350 nm) as compared to the solution (1 cm). Values for $\Delta A/F$ of 1.3 with mJ cm^{-2} and of 1.2 with 30 mJ cm^{-2} result for 308 nm irradiation (the values for 248 nm are about the same). The slightly

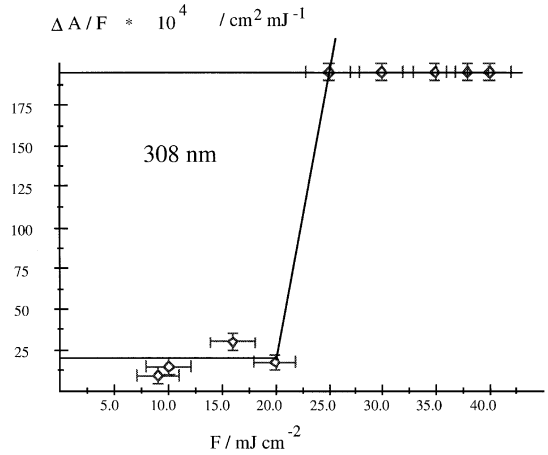

Fig. 4. Plots of the change of absorbance ΔA of thin polymer films (0.21 μm), recorded before and after single pulse irradiation with 308 nm. The values are normalized with the applied fluence and plotted vs. the fluence. A sudden increase is detected between 20 and 25 mJ cm^{-2}

larger (about 10) change of $\Delta A/F$ for 10 mJ cm^{-2} in the films is rationalized by an additional thermal decomposition of the polymer, which is caused by the exothermic photo-decomposition due to the higher density of the chromophores in condensed phase.

The absence of the sudden increase of $\Delta A/F$ in the solutions at higher fluence indicates that such an increase is the result of a solid state process due to the ablation. To prove that ablation really occurred, the samples were inspected optically after irradiation. The clean surface of the quartz wafer was detected after several pulses, showing that the polymer was completely removed during the laser irradiation.

For both irradiation wavelengths (248 and 308 nm) *new values* of F_{rh}^{new} are determined from the experiments with the thin films at low laser fluences. The *old values* F_{th}^{old}, which were derived from the linear regression according to (6) had given higher values [11]. Possible reasons for the quite large deviations are the aforementioned errors in the linear regression analysis and changes (physical and chemical) of the polymer for consecutive pulses. Another possibility for the different values is a change of the mechanism between thick films and thin films cast on quartz. The films cast on quartz have an additional interface between the polymer and quartz. An influence of internal reflection did not appear in the data. For all applied fluences linear relations between the film thickness and the transmission value were found (Fig. 1). Whether adhesion between the polymer and quartz has an influence on the ablation characteristics is not totally clear. Considering that adhesion will have the most influence on the first layer between the polymer and quartz and the fact that for our measurement polymer always remained (Fig. 2) on the quartz, suggests that adhesion has only a minor influence. Other possibilities are shock waves, reflected from the substrate and thermal heating due to absorption of the substrate. Therefore it is necessary to keep in mind that thin films might alter the ablation mechanism.

The new values, derived for the thin films, are compiled together with old values and other optical and ablation parameters in Table 1.

Threshold behavior. A closer inspection of the Figures 3 and 4 shows that a different behavior is observed for 248 nm and 308 nm irradiation. The ablation at 308 nm, where the polymer has a higher absorption coefficient (Fig. 2), shows a very clear and well-defined threshold fluence. This type of sharp threshold was previously found only for irradiation of polyimide with an ArF excimer laser (193 nm). In a study of polyimide laser ablation at various wavelengths, this behavior was assigned to a "photochemical process" [22]. In this study [22] only single pulse data were employed and the thresholds of ablation were analyzed by using the QMB technique.

The threshold at 248 nm irradiation is not clearly defined as compared to the 308 nm threshold. A description as a "threshold fluence region" [23] is more appropriate. In the fluence range from 16 to 32 mJ cm^{-2} an increase of $\Delta A/F$ is detected. The increase is exponential, followed by a constant area as shown in Fig. 3. This was also seen by Küper et al. [22] as ascribed to a "photothermal mechanism". The threshold behavior indicates that a photochemical model can be applied, at least for an irradiation with 308 nm.

Another significant characteristic of the triazeno-polymer is the difference between α_{lin} and α_{eff}, especially at 308 nm. These values differ by one order of magnitude which is unusual. Generally, only slight changes, similar values, [24] or changes in the opposite direction [25] have been reported. In the case of a higher value of α_{eff} [25] this behavior was assigned to a "significant increase of the temperature" during ablation.

One explanation for the decrease of α is chromophore saturation, which is similar to those reported for the ablation of collagen at 193 nm [26] and PI at 193 and 248 nm [16–18]. In these studies, the transmission of the laser pulse through thin polymer films was used as a probe for the dynamic target optics, which is also described with the same theoretical model we are using in this study.

Thickness dependence. Before describing the transmission behavior, the influence of the film thickness must be discussed. During the determination of the threshold fluence, an unexpected feature was detected. For both irradiation wavelengths, a dependence of $\Delta A/F$ on the film thickness was detected. At 308 nm irradiation, this is observed above the threshold fluence, and for 248 nm at the upper level of the threshold fluence range (32 mJ cm^{-2}). At fluence values of 22.5 mJ cm^{-2} at 308 nm and 32 mJ cm^{-2} at 248 nm, $\Delta A/F$ increases with increasing film thickness, whereas for the fluences below the threshold $\Delta A/F$ is independent of the film thickness.

In the case of the XeCl laser irradiation, the $\Delta A/F$ values increase with increasing film thickness to reach a maximum value as shown in Fig. 5. For 248 nm irradiation, an increase of the ratio can also be detected, but with a shallower slope, as seen in Fig. 5.

In the case of KrF laser irradiation, no clear maximum was observed within the applied range of film thickness. Thicker films could not be used because the high absorption coefficient at the maximum resulted in optical densities too large to measure.

From the UV spectra (a final curve b is shown in Fig. 2), it can be deduced that the film is not completely ablated at the applied fluence. The UV spectrum after the irradiation still shows the same absorption only with lower absorbance values.

Since α_{lin} is not valid during ablation, it must be considered that non-linear effects like chromophore saturation or decomposition of the polymer during the time scale of the pulse, occur.

Thermal and photochemical decomposition release energy and accelerate the polymer decomposition. This additional energy can lead to a higher decomposition rate than expected from the laser energy alone. Thermogravimetric analysis (TG) of the polymer showed that the exothermic decomposition starts at about 500 K [19, 20]. In the case of the photochemical decomposition, no experimental data, whether of an exo- or endothermic process, are available. However, semiempirical MO [27] calculations were conducted for a model compound (shown in scheme 2) and its fragments; the heat of formations were calculated using PM 3 Hamiltonian [28], and the UV transitions were calculated by ZINDO [29] using the INDO/1 Hamiltonian. The calculations, assuming a homolytic bond cleavage between the NN single bond

Table 1. Optical and ablation parameter of the triazeno-polymer

	248 nm irradiation	308 nm irradiation
d_{max} [μm][1]	3.2	1.3
α_{lin} [cm^{-1}]	66 000	166 000
α_{eff} [cm^{-1}][1]	41 000	18 000
F_{th}^{new} [mJ cm^{-2}]	16–32	22.5
F_{th}^{old} [mJ cm^{-2}][1]	91	114
monomer density ρ_0	$1.9 * 10^{21}$ cm^{-3}	$1.9 * 10^{21}$ cm^{-3}

[1] Ref. 11.

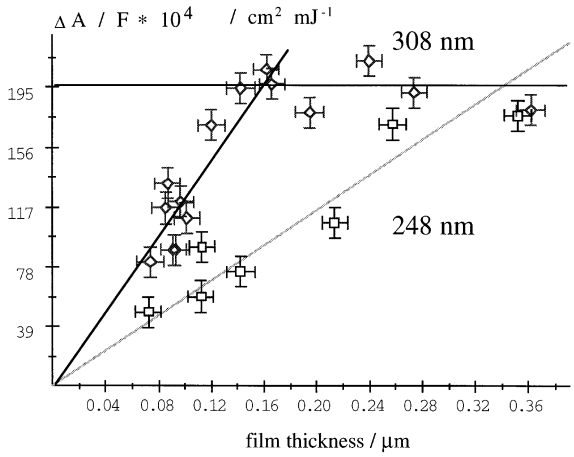

Fig. 5. Plots of the normalized change of the absorbance ($\Delta A/F$) vs. the used film thickness. At 308 nm irradiation (◇) a maximum value is reached. In the case of 248 nm irradiation (□) maximum value is reached within the applied film thickness

with a subsequent release of nitrogen, also showed an exothermic decomposition with a similar decomposition enthalpy as that measured with differential scanning calorimetry (DSC) for the thermal decomposition. The result that both decomposition pathways are exothermic gives some indication that a photothermal part in the ablation mechanism might be involved.

Calculation of the number of chromophores. One important parameter in the model is the number of chromophores. In the previous study this number was always used as an adjustable parameter in the model. In our opinion it seemed to be more correct to calculate the chromophore number independently. This would result in a better use and evaluation of the model. The most important property of the triazenopolymer is the absorption maximum around 330 nm which was assigned to the triazeno-chromophore in structural similar compounds [30, 31].

For a more detailed analysis of the absorption properties, the UV spectrum of the model compound (scheme 3), which was also synthesized, was calculated using semiempirical methods (MOPAC/ZINDO). The experimental UV spectrum of the model compound is nearly identical to the spectrum of the polymer. From the calculation it was derived that four UV transitions contributed to the absorption maximum at 330 nm. In detail, these are the HOMO → LUMO, the HOMO → LUMO + 1, the HOMO → LUMO + 2 and the HOMO → LUMO + 3 transitions. The first two orbital excitations showed a large involvement of the triazeno-group, whereas the other two are mainly localized at the phenyl moieties. Similar results were previously reported for aryl-dialkyltriazenes [31] which have the same structural unit. Starting from simple chemical considerations, it can be thought that the number of chromophores responsible for the absorbance at around 300 nm is a low value, for example 2 or 4 per unit. On the other hand, the semiempirical calculations indicated the involvement of the phenyl moieties in the absorption properties; therefore, the chromophore number in the calculation was not restricted to low values. As a starting point for the calculation, numbers close to the expected value were chosen.

In the case of the 248 nm irradiation, it is more complicated to predict a chromophore number because the absorption spectrum (Fig. 2) showed an absorption minimum around these wavelengths. Assuming a Lorentzian profile of the UV-transitions, the KrF excimer laser can excite both absorption bands, below and above 248 nm. Therefore, no indication is given whether the phenyl-system (below 248 nm) or the triazeno group (above 248 nm) will be excited.

A simple consideration of typical values for N–N bond energies are in the range of 1.5 to 3.0 eV (taken from hydrazine derivatives) [32]. Therefore, both the 248 nm (5 eV) and the 308 nm (4 eV) excimer lasers are capable of breaking of this bond directly. For aryl-dialkyl triazene compounds, which exhibit a similar structural unit, a radical pathway of decomposition was reported [30, 31, 33]. The first step in this pathway is the homolytic bond cleavage between the N–N bond, creating a labile diazo-radical which decomposes at an extremely fast rate. The fact that both applied lasers are capable of a direct bond-breaking in the polymer creates the possibility of applying a photochemical model.

2.2 Application of the Model

Transmission studies. To determine the influence of the optical dynamic properties on the high etch rate at 308 nm, the transmission of the laser pulse through thin polymer films was measured.

The ratio of T_H/T_L as suggested by Pettit et al. [18] was plotted against the laser fluence. For 248 nm irradiation, only fluence values up to about 800 mJ cm^{-2} could be used because at higher fluences (e.g. 1.1 J cm^{-2}) ablation of the quartz occurs. For the same reason, the upper fluence limit for 308 nm irradiation is about 2.5 J cm^{-2}. These values are in rough agreement with studies of the ablation of silica [34, 35] which also showed a strong dependence of the ablation on the surface quality [35].

For the 308 nm irradiation, a clear increase of the transmission ratio starting at about 120 mJ cm^{-2} is derived (shown in Fig. 6). For 248 nm, only a slight increase is found (shown in Fig. 7) although this could be due to the limited fluence range. The dynamic optical behavior of the polymer can provide a preliminary explanation as to the difference of the experimental etch rates compared with the expectation from the linear absorption coefficient and the prediction from equation (1).

The etch rates of the polymer together with the predicted values (from (1), dash dot line) are shown in Fig. 8 and 9 for both irradiation wavelength.

In the case of 308 nm irradiation, the difference between the experimental data and values predicted by

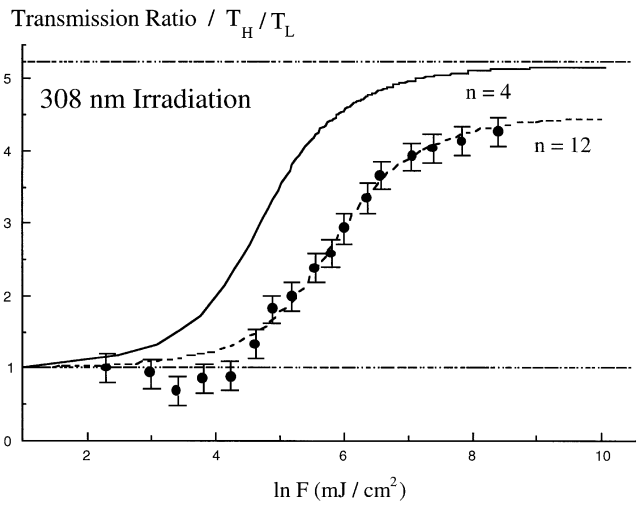

Fig. 6. Transmission ratio (high fluence transmission/low fluence transmission) vs. laser fluence at 308 nm. The discrete data points indicate the experimental results. The linear behavior is indicated with the line at $T_H/T_L = 1$, whereas the line at $T_H/T_L = 5.26$ indicates the theoretical maximum value for the transmission ratio according to (7). The *solid* curve is the result of applying the fit parameter of Fig. 8, which gives a satisfying result for the ablation rate. The *dashed* line shows the result of a fit which gives better results for T_H/T_L

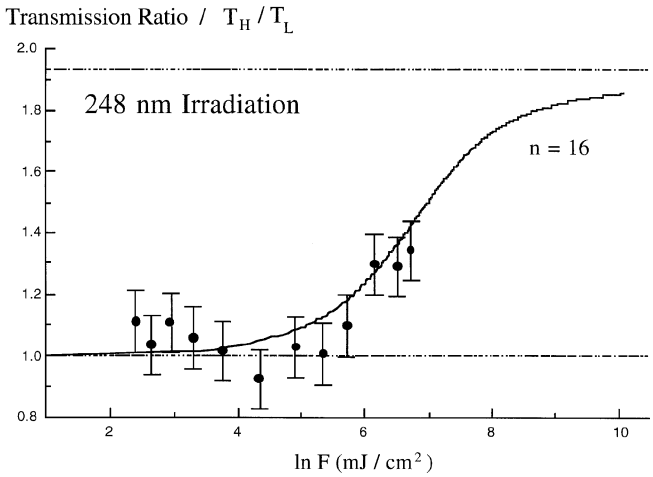

Fig. 7. Transmission ratio (high fluence transmission/low fluence transmission) vs. laser fluence at 248 nm. The discrete data points indicate the experimental results. The linear behavior is indicated with the line at $T_H/T_L = 1$, whereas the line at $T_H/T_L = 1.95$ indicates the theoretical maximum value for the transmission ratio according to (7). The *solid* curve is the result of applying the fit parameter of Fig. 9, which gives a satisfying result for the ablation rate

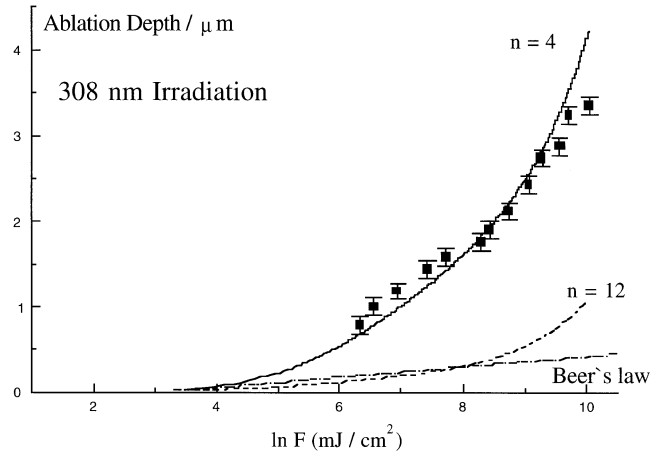

Fig. 8. Ablation depth vs. pulse fluence relationship for the 308 nm XeCl excimer laser irradiation of a 200 μm thick polymer film. The experimental data are taken from [11]. The *dash-dot* curve indicates the predicted relationship based on Beer's law. The *continuous* curve uses $n = 4$ to reach a satisfying fit. The *dash* curve show the result of different fit parameter, $n = 12$, which must be used to reach a satisfying fit of the transmission ratio in Fig. 6

Beer's law is much higher than in the case of 248 nm. Also, the increase of the transmission ratio T_H/T_L vs. fluence at 308 nm exceeds that at 248 nm, showing that the target's dynamic optical properties could explain the experimental etch rates.

To obtain a more detailed understanding of the dynamic process, the theoretical model of Pettit et al. [18] was applied to the experimental data of the triazenopolymer.

It was not possible to obtain satisfying fits to the experimental data using the single photon treatment and equations (1) and (2) [17, 18], therefore, the two-level absorption model was used. Equation 3 may be solved numerically using a fourth order Runge–Kutta method. The results of numerically integrating (3) were compared to the exact solution for the single photon absorption, $\sigma_2 = 0$, (1) and (2) to benchmark the solution method. The two calculated transmission ratios agreed to within $< 0.1\%$, but the ablation depths varied by as much as about 10%. This is not surprising since (3) is a direct function of S but not of x.

308 nm irradiation. For both data sets, etch rate and transmission ratio T_H/T_L, the two-level model must be applied. With this model, it was possible to obtain a good fit of the ablation rate up to a fluence range of about $20\,\mathrm{J\,cm^{-2}}$ as shown in Fig. 8 for the polymer films with a thickness of about 200 μm. For this fit, values for $\rho = 7.60 * 10^{21}\,\mathrm{cm^{-3}}$, $\sigma_1 = 2.184 * 10^{-17}\,\mathrm{cm^2}$, $\sigma_2 = 1.420 * 10^{-19}\,\mathrm{cm^2}$ were used which correspond to a chromophore number (n) of 4. These values are consistent with the values discussed previously. The result of this fit is shown as the solid curve in Fig. 8, where the etch rate based on Beer's law is also included. This line is obviously much lower than the experimental values. Unfortunately, it was not possible to use the same set of fitting parameters for the transmission ratio. The fit with $n = 4$, shown in Fig. 6 by the solid line, increases much earlier (close to $10\,\mathrm{mJ\,cm^{-2}}$) than the measured values, and nearly reaches the theoretical maximum value. This value is calculated from (7)

$$\left.\frac{T_H}{T_L}\right|_{\max} = \frac{1}{e^{-\sigma_{lin} d}} = e^{\sigma_{lin} d} \tag{7}$$

and is indicated in Fig. 6 with the dash-dot-dot line at 5.26. The discrepancy, especially at the point where the curve increases, is not due to a bleaching of the film during the measurement of T_L. This would lead to lower values of the transmission ratio as compared to the true film transmission. This is stated as one possible reason for deviations in Ref. [18]. The energy of the UV spectrometer which is used to determine T_L is clearly much lower (around $0.2\,\mu\mathrm{J\,cm^{-2}}$) [36] than the value used in Ref. [18] ($2\,\mathrm{mJ\,cm^{-2}}$). It is very unlikely that such a low value would bleach the film. To achieve a satisfying fit (dashed line) of the transmission ratio, it was necessary to change the parameters to $\rho = 2.28 * 10^{22}\,\mathrm{cm^{-3}}$, $\sigma_1 = 7.281 * 10^{-18}\,\mathrm{cm^2}$, $\sigma_2 = 6.917 * 10^{-19}\,\mathrm{cm^2}$ which correspond to 12 chromophores. This value would also be consistent with the possible number of chromophores, as discussed previously. Unfortunately, the etch rate with these values results in a curve (dashed line in Fig. 6) close to the curve predicted by Beer's law, which is also much too low.

Further attempts of fitting both experimental curves showed that the necessary parameters always follow opposite trends.

A multiphoton absorption process as described by Pettit et al. [16, 17], which was successfully applied for the ablation of teflon with femtosecond pulses at 248 nm [17] and 798 nm [37], was not considered in this case. The two reasons are the high absorption coefficient and the detected bleaching of the absorption in the transmission ratio, whereas a multiphoton process would increase the

absorption. Whether a cyclic multiphoton process [38] described for anthracene doped PMMA can be responsible for this different behavior will be the subject of further studies. During this process, the excited triplet states play the key role; therefore, transient absorption spectra will give valuable information. For a similar polymer where only the bridging atom between the phenylring is changed, time dependent measurements have already given valuable information [39]. According to these results the bleaching detected in the transmission studies can also be ascribed to the polymer decomposition during the time scale of the pulse (in this case 351 nm irradiation is used) [39]. In further studies, the influence of thermal aspects must be included in the mechanism of ablation at 308 nm.

248 nm irradiation. Contrary to the results at 308 nm, it was possible to fit the etch depth (Fig. 9) as well as the transmission ratio (Fig. 7) with one set of parameters.

As for 308 nm irradiation it was not possible to use the one photon absorption model, therefore again the two level model was applied. The parameters for the fit are $\rho = 3.04 * 10^{22}\,\mathrm{cm}^{-3}$, $\sigma_1 = 2.171 * 10^{-18}\,\mathrm{cm}^2$, $\sigma_2 = 1.085 * 10^{-18}\,\mathrm{cm}^2$. This is equal to 16 chromophores. The value of chromophores is again in the expected and reasonable range for the involvement of the phenyl moieties in the absorption. The result is shown as the solid curve in Fig. 7. Again, the maximum theoretical value is included as a dash-dot-dot line. Additionally, it should be stated that the data set for the transmission ratio is very limited, and that the Beer's law absorption (dash-dot line in Fig. 9) gave at least a similar result as the fit. For the linear fit, the deviation is mainly in the higher fluence range, whereas for the transmission study a slight increase in the transmission is found. Nevertheless in the case of 248 nm irradiation, the fit with one set of parameters shows agreement with both sets of experimental data.

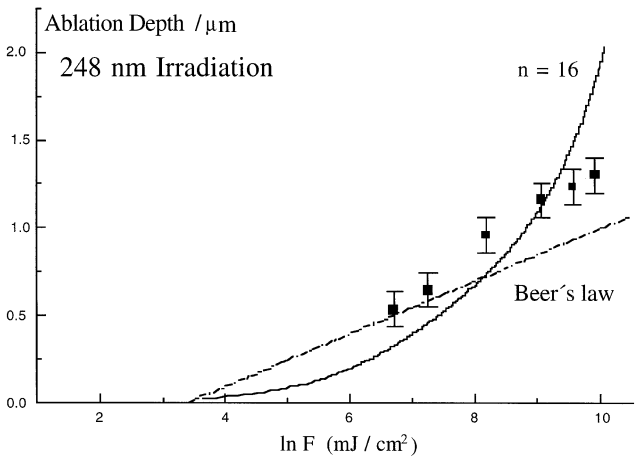

Fig. 9. Ablation depth vs. pulse fluence relationship for irradiation of a 200 µm thick polymer film with the KrF excimer laser (248 nm). The experimental data are taken from [11]. The two curves are plotted over a large fluence range. The *dash-dot* curve indicates the predicted relationship based on Beer's law. The *continuous* curve is the result of the two level absorption model, using the same fit parameter (n) as in Fig. 7. The parameter is described in the text

This may be an indication, together with the different threshold behavior as compared to 308 nm irradiation, that there are different mechanisms acting at the different laser wavelengths, and that the concept of designing polymers for special laser wavelength is working.

3 Conclusion

The study of the triazenopolymer showed a clearly defined threshold fluence at 308 nm, whereas with 248 nm irradiation a "threshold fluence region" is determined. Films with different thickness exhibit a dependence of the change of the absorbance on the film thickness. The fluence-normalized change of the absorbance, $\Delta A/F$, increases with increasing film thickness, to reach, in the case of 308 nm, a constant value. For 248 nm irradiation, a maximum value can not be reached because of the limited range of film thickness which can be studied. The lack of correlation between the thickness where the value becomes constant and the linear absorption coefficient shows that even at such low fluences α_{lin} is not valid during ablation or that thermal decomposition takes place.

The transmission for ns UV pulses is clearly dependent on the fluence in a range of a few $\mathrm{mJ\,cm}^{-2}$ to several $\mathrm{J\,cm}^{-2}$. With 248 nm irradiation, only a slight increase of the transmission ratio $T_{\mathrm{H}}/T_{\mathrm{L}}$ could be detected, whereas with the XeCl excimer laser irradiation much higher transmission ratio values are reached which are close to the theoretical limit.

Again there is a significant difference between the irradiation at 248 nm and 308 nm. The two-level model of Pettit et al. [18] can only describe the behavior with both sets of data for 248 nm irradiation but not for the 308 nm irradiation. In the latter case, it is possible to reach a satisfactory fit to either the etch rate or the transmission ratio but unfortunately not to both sets of data. Taken together, this demonstrates that it was not possible to apply the photochemical model to a triazenopolymer, which is known to be photolabile. This suggests that additional parameters, such as decomposition enthalpy, should be considered. Therefore it is probably impossible to separate the ablation mechanism into photochemical or photothermal. The mechanism will always be a mixture of both, with a variable contribution of the photochemical and photothermal part, depending on the polymer.

Acknowledgements. T.L. expresses his gratitude to the A.v. Humboldt Foundation and to the Science Technology Agency (STA) of Japan for a research fellowship.

References

1. Y. Kawamura, K. Toyoda, S. Namba: Appl. Phys. Lett., **40**, 374 (1982)
2. R. Srinivasan, V. Mayne-Banton: Appl. Phys. Lett., **41**, 578 (1982)
3. S. Lazare, V. Granier: Laser Chem., **10**, 25 (1989)
4. R. Srinivasan, B. Braren: Chem. Rev., **89**, 1303 (1989)
5. R. Iscoff: Laser and Optronics, **6**, 65 (Nov. 1987)
6. J.M. Isner, P.G. Steg, R.H. Clarke: IEEE J. Quant. Electr., **QE-23**, 482 (1986)

7. H. Nornes, R. Srinivasan, R. Solanski, E. Johnson: Soc. Neurosci., **11**, 1167 (1985)
8. R.J. Lane, R. Linsker, J.J. Wynne, A. Torres, R.G. Geronemus: Arch. Dermatol., **121**, 609 (1985)
9. Y.S. Liu, H.S. Cole, H.R. Philipp, R. Guada: *SPIE-Proceedings 774*, 155 (1987)
10. K. Jain: *Excimer Laser Lithography*, SPIE. The International Society for Optical Engineering, Bellingham, 1990
11. T. Lippert, J. Stebani, J. Ihlemann, O. Nuyken, A. Wokaun: Angew. Makromol. Chem., **206**, 97 (1993)
12. T. Lippert, J. Stebani, J. Ihlemann, O. Nuyken, A. Wokaun: J. Phys. Chem., **97**, 12296 (1993)
13. S.R. Cain, F.C. Burns, C.E. Otis: J. Appl. Phys., **71**, 4107 (1992)
14. N.P. Furzikov: Appl. Phys. Lett., **56**, 1638 (1990)
15. G.C.D'Couto, S.V. Babu: J. Appl. Phys., **76**, 3052 (1994)
16. G.H. Pettit, R. Sauerbrey: Appl. Phys. Lett., **58**, 793 (1991)
17. G.H. Pettit, R. Sauerbrey: Appl. Phys. A **56**, 51 (1993)
18. G.H. Pettit, M.N. Ediger, D.W. Hahn, B.E. Brinson, R. Sauerbrey: Appl. Phys. A **58**, 573 (1994)
19. J. Stebani, T. Lippert, O. Nuyken, A. Wokaun: Makromol. Chem., Rapid. Commun., **14**, 365 (1993)
20. A.N.K. Lau, L.P. Vo: Macromolecules **25**, 7294 (1992)
21. S. Lazare, J.C. Soulignac, P. Fragnaud: Appl. Phys. Lett., **50**, 624 (1987)
22. S. Küper, J. Brannon, K. Brannon: Appl. Phys. A **56**, 43 (1993)
23. L.G. Reyna, J.R. Sobehart: J. Appl. Phys., **76**, 4367 (1994)
24. J.H. Brannon, J.R. Lankard, A.I. Baise, F. Burns, J. Kaufmann: J. Appl. Phys., **58**, 2036 (1985)
25. J.E. Andrew, P.E. Dyer, D. Foster, P.H. Key: Appl. Phys. Lett., **43**, 717 (1993)
26. G.H. Pettit, M.N. Ediger, R.P. Weiblinger: Appl. Opt., **32**, 488 (1993)
27. J.J.P. Stewart: *MOPAC*, Programm 455, Quantum Chemistry Programm Exchange, University of Indiana, Bloomington, IN
28. J.J.P. Stewart: J. Comput. Chem., **10**, 209, 221 (1989), J.J.P. Stewart, J. Comput Aided Mol. Design, **4**, 1 (1990)
29. ZINDO: Prof. M.C. Zerner Intermediate Neglect of Differential Overlap Programm, University of Florida Quantum Theory Project
30. T. Lippert, J. Stebani, O. Nuyken, A. Wokaun: J. Photochem. Photobiol. A: Chem., **78**, 139 (1994)
31. J.-C. Pantiz, T. Lippert, J. Stebani, O. Nuyken, A. Wokaun: J. Phys. Chem., **97**, 5246 (1993)
32. R. Shaw: in *The Chemistry of the Hydraze Azo and Azoxy Groups*, Ed., S. Patai, John W Wiley & Sons, 1975, p. 62
33. A. Stasko, V. Adamcik, J. Stebani, O. Nuyken, T. Lippert, A. Wokaun: Makromol. Chem., **194**, 3385 (1993)
34. B. Braren, R. Srinivasan: J. Vac. Sci., B **6**, 537 (1988)
35. J. Ihlemann, B. Wolff, P. Simon: Appl. Phys. A **54**, 363 (1992)
36. Shimadzu Corporation, private communication
37. H. Kunagai, K. Midorikawa, K. Toyoda, S. Nakamura, T. Okamoto, M. Obara: Appl. Phys. Lett., **65**, 1850 (1994)
38. H. Fukumura, H. Masuhara: Chem. Phys. Lett., **221**, 373 (1994)
39. H. Furutani, H. Fukumura, H. Masuhara, T. Lippert: unpublished results